JDI Journal of Diabetes Investigation Open access
Official Journal of the Asian Association for the Study of Diabetes
ORIGINAL ARTICLE

# Circular ribonucleic acid nucleoporin 98 knockdown alleviates high glucose-induced proliferation, fibrosis, inflammation and oxidative stress in human glomerular mesangial cells by regulating the microribonucleic acid-151-3p–high mobility group AT-hook 2 axis

Qianlan Dong[1], Longhao Dong[2], Yanting Zhu[1], Xiaoming Wang[1], Zhenjiang Li[1], Linping Zhang[1]*

[1]Kidney Disease and Dialysis Center, Shaanxi Provincial People's Hospital, Xi'an, Shaanxi, China, and [2]Department of Emergency, Tongchuan People's Hospital, Tongchuan, Shaanxi, China

**Keywords**
Circular ribonucleic acid nucleoporin 98, High mobility group AT-hook 2, Microribonucleic acid-151-3p

***Correspondence**
Linping ZhangTel.: +86-29-8525-1331
E-mail address: linping0117@163.com

*J Diabetes Investig* 2022; 13: 1303–1315

doi: 10.1111/jdi.13821

## ABSTRACT

**Aims/Introduction:** This study aimed to investigate the role and mechanism of circular ribonucleic acid nucleoporin 98 (circNUP98) in diabetic nephropathy (DN).

**Materials and Methods:** Human glomerular mesangial cells (HMCs) were stimulated with high glucose (HG) to imitate the growth environment of cells under the DN condition. Levels of genes and proteins were tested by quantitative reverse transcription polymerase chain reaction and western blot. Cell proliferation, apoptosis and inflammatory response were analyzed by using cell counting kit-8, flow cytometry and enzyme-linked immunosorbent assay analysis, respectively. Oxidative stress and fibrosis were evaluated by detecting the activity of reactive oxygen species, malondialdehyde, superoxide dismutase, fibronectin and collagen IV. The binding interaction between microribonucleic acid (miR)-151-3p and high mobility group AT-hook 2 (HMGA2) or circNUP98 was confirmed using dual-luciferase reporter, pull-down and ribonucleic acid immunoprecipitation assays. Exosomes were isolated by ultracentrifugation, and qualified by transmission electron microscopy, nanoparticle tracking analysis and western blot.

**Results:** CircNUP98 expression was higher in the serum of DN patients and HG-stimulated HMCs. Functionally, circNUP98 knockdown alleviated HG-induced proliferation, fibrosis, inflammatory response and oxidative stress in HMCs. Mechanistically, circNUP98 directly sponged miR-151-3p, which targeted HMGA2. Rescue experiments showed that miR-151-3p reversed the inhibitory effects of circNUP98 knockdown on HG-induced HMC dysfunction. Furthermore, miR-151-3p re-expression also led to an inhibition of the aforementioned biological behaviors, which was attenuated by HMGA2 upregulation. Besides that, CircNUP98 was found to be packaged into exosomes of DN, and exosomal circNUP98 possessed diagnostic value for DN patients.

**Conclusion:** CircNUP98 knockdown alleviates HG-induced proliferation, fibrosis inflammation and oxidative stress in HMCs by regulating the miR-151-3p–HMGA2 axis, which might provide a potential approach for DN therapeutics.

Received 6 January 2022; revised 27 March 2022; accepted 27 April 2022

## INTRODUCTION

Diabetic nephropathy (DN), one of the chronic microvascular complications of diabetes mellitus, represents the major cause of end-stage renal failure throughout the world[1]. The most significant pathological changes of clinical DN patients are the glomerular lesions, which are, especially, thickened glomerular basement membrane and mesangial dilatation[2, 3]. Furthermore, the active proliferation and extracellular matrix (ECM) accumulation in renal glomerular mesangial cells (MCs) is one of the significant pathological characteristics of DN[4]. During diabetes, MCs are exposed to a high-glucose (HG) condition, which leads to ectopic expression of fibroin and cytokines, resulting in renal fibrosis in return[5]. Thus, further investigation on HG-induced MC injury is of great significance for DN therapy.

Circular ribonucleic acids (circRNAs) are a class of non-coding RNAs with a covalently closed loop formed by back-splicing, which renders them resistant to RNaseR digestion[6]. Furthermore, circRNAs are widely expressed across various species, and show high stability, and are specific and highly organized relative to other types of RNA[7]. In addition, researchers have shown that circRNAs play crucial roles in regulating cellular biological processes[8–10]. Thus, disease-specific expression of circRNAs are considered as promising therapeutic and diagnostic molecular markers for the clinical diseases[11]. Recently, a growing number of studies have shown that aberrantly expressed circRNAs were enrolled in the evolution of DN[12]. For example, circRNA_15698 contributed to the synthesis of ECM-related protein collagen type I, IV and fibronectin by promoting transforming growth factor-β1 through miR-185[13]. Peng *et al.* showed that circRNA_010383 suppressed HG-evoked ECM accumulation *in vitro*, and restrained renal fibrosis and proteinuria in a DN mice model[14]. CircRNA nucleoporin 98 (NUP98; circNUP98, ID: hsa_circ_0000274) is derived from its host gene, *NUP98*. It locates at chr11: 3752620–3,774,638 with the length of 556 bp. A recent study suggested that circNUP98 predicted a poor prognosis of renal cell carcinoma patients, and promoted cell growth in renal cell carcinoma by the miR-567–PRDX3 axis[15]. However, the biological function and potential value of circNUP98 in the DN process remain vague.

Here, the present study used HG-stimulated human MCs (HMCs) to investigate the function of circNUP98 in cell proliferation, ECM production, inflammation and oxidative stress. In addition, how circNUP98 regulates these behaviors was also explored, which might provide a potential approach for DN therapeutics.

## MATERIALS AND METHODS

### Blood collection

The blood samples (5 mL) were collected from 33 patients with clinically diagnosed DN, and 30 sex- and age-matched physiologically normal individuals ($n$ = 33) at Shaanxi Provincial People's Hospital, Xi'an, Shaanxi, China. Then serum samples were obtained by centrifugation at 3,000 $g$ for 10 min. Clinical characteristics of all individuals are shown in Table 2. This work was approved by the Ethics Committee of Shaanxi Provincial People's Hospital, and manipulated in line with the Declaration of Helsinki. All the participants gave written informed consent.

### Cell culture and treatment

HMCs were obtained from Cell Bank of Shanghai Institute of Cell Biology (Shanghai, China), and then grown in Dulbecco's modified Eagle's medium (Invitrogen, Carlsbad, CA, USA) harboring 10% fetal bovine serum (Invitrogen) and 1% penicillin–streptomycin (Solarbio, Shanghai, China) with 5% CO2 at 37°C.

For glucose treatment, HMCs at 80% confluence were stimulated with 30 mmol/L D-glucose (Solarbio) for different times, and we found that circNUP98 expression was much higher in HMCs when treated with high glucose for 24 h (Figure S1a). Then cells were exposed to 30 mmol/L D-glucose for 24 h to mimic the growth environment of HMCs under the DN condition (HG group). The cells treated with D-glucose at 5 mmol/L served as the control (NG group).

### Quantitative real-time polymerase chain reaction

TRIzol reagent (Life Technologies, Carlsbad, CA, USA) was used to isolate total RNAs. Next, approximately 3 μg of total RNA was reversely transcribed into complementary deoxyribonucleic acid using the PrimeScript RT reagent kit (Takara, Dalian, China) or TransStart Top Green qPCR SuperMix (TransGen Biotech, Beijing, China), and then quantitative reverse transcription polymerase chain reaction (qRT–PCR) was carried out using SYBR Premix Ex TaqII (Takara). The cycle threshold value of genes was normalized to β-actin or U6. The primer sequences are listed in Table 1.

**Table 1** | Primers sequences used for quantitative reverse transcription polymerase chain reaction

| Name | | Primers for qRT-PCR (5′-3′) |
|---|---|---|
| circNUP98 | Forward | TGGGCTGGATGACGATGAAC |
| | Reverse | CCCAAAGGCTCCTGTACCAA |
| HMGA2 | Forward | TCTGCCGAAGAGGACTAGGG |
| | Reverse | ACTGCAGTGTCTTCTCCCTTC |
| NUP98 | Forward | CCGTGATACCGAAGTTGAAAGC |
| | Reverse | AGATGCCTGCAAGACCTCAC |
| miR-151-3p | Forward | GGATGCTAGACTGAAGCTCCT |
| | Reverse | CAGTGCGTGTCGTGGAGT |
| β-Actin | Forward | GGCACTCTTCCAGCCTTCC |
| | Reverse | GAGCCGCCGATCCACAC |
| U6 | Forward | GCTTCGGCAGCACATATACTAAAAT |
| | Reverse | CGCTTCACGAATTTGCGTGTCAT |

circNUP98, Circular ribonucleic acid nucleoporin 98; HMGA2, high mobility group AT-hook 2; miR-151-3p, microribonucleic acid-151-3p; qRT-PCR, quantitative reverse transcription polymerase chain reaction.

### Actinomycin D treatment and RNase R digestion

For actinomycin D treatment, HMCs were placed on a 24-well plate overnight and then incubated with 5 μg/mL actinomycin D. The levels of circNUP98 and linear NUP98 were determined by qRT–PCR.

For RNase R treatment, approximately 3 μg of total RNAs were mixed with 5 U/μg of RNase R (Epicenter Biotechnologies, Madison, WI, USA) for 3 h at 37°C, then the levels of circNUP98 and linear NUP98 were measured by qRT–PCR.

### Cell transfection

The small interfering (si)RNAs targeting for circNUP98 (si-circNUP98) and non-target siRNA (si-NC), miR-151-3p mimic (miR-151-3p), inhibitor (anti-miR-151-3p), and the negative control (NC; miR-NC or anti-NC) were synthesized by Genema (Shanghai, China). The full-length HMGA2 was cloned into pcDNA3.1 (Invitrogen) to overexpress HMGA2 (with empty pcDNA3.1 as the NC (vector). Then, the plasmids or oligonucleotides were introduced into HMCs transiently. After confirming the transfection efficiency, HMCs were subjected to HG or NG treatment for subsequent analysis.

### Cell counting kit-8 assay

HMCs were seeded in 96-well plates, and incubated with 90 μL/well of fresh medium containing 10 μL/well of cell counting kit-8 solution for 2 h. At 0, 24, 48 and 72 h, the absorbance of the medium at 450 nm was examined to evaluate cell proliferation.

### Flow cytometry

HMCs were stained with FITC-conjugated anti-annexin V antibody and propidium iodide for 15 min according to the manufacturer's instruction. The percentage of apoptotic cells were then measured by FACSCalibur flow cytometry (Biosciences, San Jose, CA, USA).

### Western blot

The proteins were isolated by using a radioimmunoprecipitation assay buffer (Beyotime, Nantong, China), then protein concentration was determined by a bicinchoninic acid protein assay kit (Beyotime). Thereafter, total protein (30 μg) was separated by 10% SurePAGE (Genscript, Nanjing, China), and protein electrophoresis membrane was transferred. Next, the membranes were incubated with the primary antibodies at 4°C overnight after blocking with 5% non-fat milk for 1.5 h. After incubation with horseradish peroxidase-conjugated secondary antibody with a 1:2,000 dilution at 37°C for 1 h, the membranes were examined using ECL reagents (Beyotime), and bands densities were analyzed by ImageJ software (National Institutes of Health, Bethesda, MD, USA). The primary antibodies included: TSG101 (1:5000, ab125011), CD81 (1: 2000, ab109201), CD63 (1:2000, ab68418), fibronectin (FN; 1:1000 ab2413), collagen IV (Col IV; ab6586), HMGA2 (1:1000, ab97276), Bcl-2 (1:2000), cleaved-caspase 3 (1:2000, ab2302) and β-actin (1:1000, ab6276) obtained from Abcam (Cambridge, MA, USA).

### Enzyme-Linked immunosorbent assay

The cell culture supernatant of HMCs was collected, and then levels of interleukin-6 (IL-6), IL-1β or tumor necrosis factor-α (TNF-α) were detected by corresponding commercial ELISA kits provided by Abcam.

### Reactive oxygen species detection

Dihydroethidium staining was used to detect intracellular reactive oxygen species (ROS) levels in HMCs. Briefly, HMCs were seeded in six-well plates with 10 μmol/L of dihydroethidium and incubated for 30 min at 37°C under darkness. After washing with phosphate-buffered saline, fluorescence intensity was determined by a fluorescence microscope at the wavelength 535/610 nm (Olympus, Tokyo, Japan) and quantified by using ImageJ analysis software to evaluate ROS production.

### Detection of malondialdehyde and superoxide dismutase activity

Cell supernatant was collected from HMCs by centrifugation at 4000 *g* for 10 min, then the content of malondialdehyde (MDA) and superoxide dismutase (SOD) in the supernatant of cell medium were measured by respective enzyme-linked immunosorbent assay kits (Beyotime) as per of the manufacturer's protocols, and analyzed by a microplate reader.

### Subcellular fractionation

Cytoplasmic and nuclear RNA isolation in HMCs was implemented in line with the instruction of the PARIS kit (Life Technologies). After elution, nuclear and cytoplasmic RNA was collected, and the circNUP98 level were detected by qRT–PCR with glyceraldehyde 3-phosphate dehydrogenase or U6 as the cytoplasmic or nuclear control transcript.

### Dual-luciferase reporter assay

CircNUP98 or HMGA2 fragments covering wild-type binding sites in miR-151-3p and the mutated sequences without miR-151-3p binding sites provided by Genema were amplified and inserted into the pmirGLO report luciferase vector (Promega, Fitchburg, WI, USA). Thereafter, the reporter plasmids together with miR-151-3p mimic or mimic NC were co-transfected into HMCs. A total of 48 h later, the relative luciferase activity was determined by dual-luciferase reporter assay kit (Promega).

### Pull-down assay

Biotin-labeled circNUP98 probe (Bio-circNUP98) and the control probe (bio-NC) were synthesized by Genepharma (Shanghai, China). HMCs cells were transfected with biotin-coupled probes, then the lysates were incubated with Dynabeads M-280 Streptavidin (Invitrogen) overnight at 4°C. The pull-down product was then analyzed by qRT–PCR after purification.

### RNA immunoprecipitation assay

RNA immunoprecipitation (RIP) assay was carried out by Magna RIP RNA Binding Protein Immunoprecipitation Kit (Millipore, Billerica, MA, USA). HMCs were lysed in RIP lysis buffer, and then incubated with magnetic beads bounded with human anti-Ago2 antibody or negative control immunoglobulin G for 2 h. The beads were incubated with proteinase K buffer, then qRT–PCR was used to detect the levels of circNUP98 and miR-151-3p.

### Isolation and identification of exosome

The collected serum were centrifuged at 3000 g for 15 min to eliminate cells and cellular debris, and then incubated with a quarter volume of Exoquick exosome precipitation solution (System Biosciences, Mountain View, CA, USA). A total of 24 h later, the mixture was subjected to centrifugation at 1,500 *g* for 30 min, and exosomes were collected after removing the supernatant. Next, the exosome pellets were resuspended in 100 μL phosphate-buffered saline for morphology observation by a transmission electron microscopy (FEI, Hillsboro, OR, USA; ×200). The size distribution of exosomes were determined using nanoparticle-tracking analysis. The exosomes marker (TSG101, CD63,and CD81) was detected by western blot analysis.

### Statistical analysis

The results in the bar graphs were expressed as mean ± standard deviation. The Student's -test (two-sided) or analysis of variance was used to evaluate group difference. All statistical analyses were carried out with GraphPad Prism 6.0 software (GraphPad, San Diego, CA, USA) with $P < 0.05$ as statistical differences.

## RESULTS

### CircNUP98 is highly expressed in DN patients and HG-stimulated HMCs

To explore the clinical value of circNUP98 in DN, the blood samples from 33 DN patients and 30 matched physiologically normal individuals were collected. Compared with the normal controls, DN patients showed higher systolic blood pressure, diastolic blood pressure, triglyceride, fasting blood glucose, glycated hemoglobin and albuminuria, and lower estimated glomerular filtration rate (Table 2). Then, the expression profile of circNUP98 was first investigated. As shown in Figure 1a, circNUP98 expression was higher in the serum of DN patients than those in normal controls. Next, circNUP98 expression on D-glucose stimulation was explored. As expected, circNUP98 was highly expressed in HMCs subjected to HG treatment for 24 h compared with NG treatment (Figure 1b). Subsequently, the circular characteristics of circNUP98 were analyzed. The results of actinomycin D treatment showed that the half-life of circNUP98 exceeded 16 h, whereas that of linear NUP98 mRNA was approximately 8 h (Figure 1c). Furthermore, RNase R treatment showed that circNUP98 could resist degradation by RNase R relative to the linear NUP98 (Figure 1d). In all, circNUP98 was an abundant and stable circRNA, and might be associated with DN progression.

**Table 2** | Clinical features of the patients with diabetic nephropathy and normal controls

| | Normal ($n$ = 33) | DN ($n$ = 33) | $P$-value |
|---|---|---|---|
| Men/women | 15/18 | 16/17 | 0.805 |
| Age (mean ± SD) | 52.40 ± 7.10 | 53.50 ± 6.80 | 0.523 |
| Disease duration (years) | – | 8.95 ± 3.72 | |
| BMI (kg/m$^2$) | 22.22 ± 3.84 | 24.43 ± 4.16 | 0.224 |
| SBP (mmHg) | 107.27 ± 7.69 | 129.87 ± 11.85 | <0.001* |
| DBP (mmHg) | 80.54 ± 5.25 | 84.22 ± 6.62 | 0.015* |
| Total cholesterol (mg/dL) | 176.54 ± 23.55 | 187.47 ± 28.73 | 0.096 |
| Triglyceride (mg/dL) | 152.62 ± 11.71 | 159.74 ± 13.45 | 0.025* |
| FBG (mmol/L) | 4.92 ± 1.33 | 7.97 ± 2.24 | <0.001* |
| HbA1c (%) | 5.88 ± 0.62 | 8.63 ± 1.18 | <0.001* |
| eGFR (mL/min/1.73 m$^2$) | 101.72 ± 11.53 | 66.81 ± 20.42 | <0.001* |
| Albuminuria (mg/24 h) | 9.35 ± 2.57 | 164.52 ± 49.62 | <0.001* |

*$P < 0.05$, compared with normal controls. BMI, body mass index; DBP, diastolic blood pressure; DN, diabetic nephropathy; eGFR, estimated glomerular filtration rate; FBG, fasting blood glucose; HbA1c, glycated hemoglobin; SBP, systolic blood pressure; SD, standard deviation.

### CircNUP98 knockdown suppresses proliferation and fibrosis in HG-induced HMCs

To further investigate the biological function of circNUP98 in HG-induced HMCs, siRNA targeting circNUP98 was designed and transfected into HMCs to knock down circNUP98. The decrease of circNUP98 expression in HMCs after si-circNUP98 suggested transfection efficacy (Figure 2a). After treatment with HG, we also observed that si-circNUP98 introduction could reduce HG-induced elevation of circNUP98 in HMCs, as expected (Figure S1b). Next, cell counting kit-8 assay and flow cytometry showed that HG treatment induced proliferation (Figure 2b) and suppressed apoptosis (Figure 2c,d) in HMCs, which were reversed by circNUP98 knockdown. Furthermore, western blot analysis suggested that circNUP98 knockdown led to an increase of anti-apoptotic protein Bcl-2, and a decrease of pro-apoptotic protein cleaved-caspase 3 in HG-induced HMCs (Figure 2e). In addition, we also observed that circNUP98 knockdown attenuated HG treatment-evoked elevation of profibrotic markers, FN and Col IV (Figure 2f). These results confirmed that circNUP98 knockdown reversed HG-induced apoptosis arrest and fibrosis in HMCs.

### CircNUP98 knockdown suppresses inflammatory response and oxidative stress in HG-induced HMCs

The role of circNUP98 on HG-induced inflammatory response and oxidative stress in HMCs was then explored. As shown in Figure 3a–c, circNUP98 silenced the levels of TNF-α, IL-6 and IL-1β in HG-stimulated HMCs. Meanwhile, we found that the

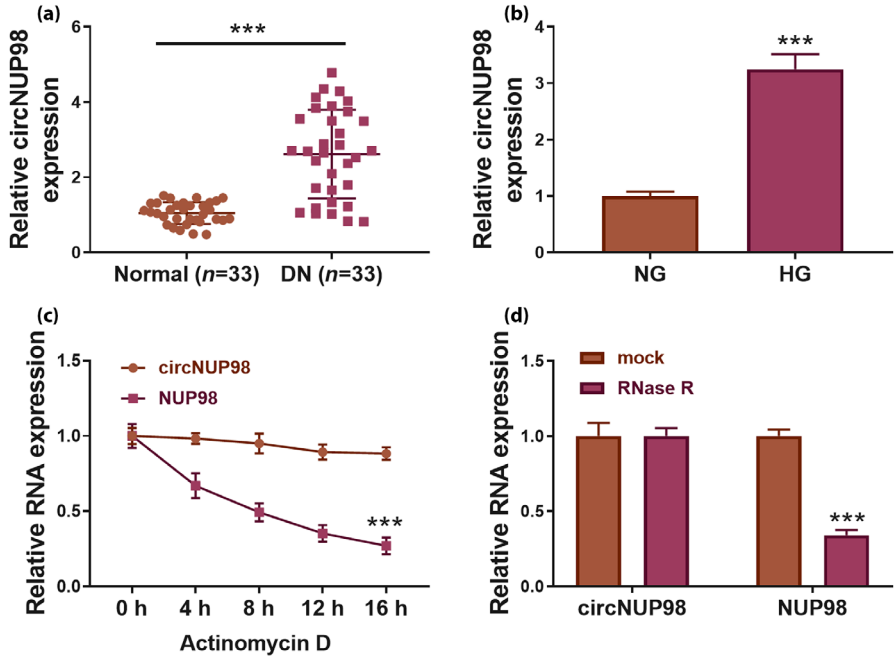


**Figure 1** | Circular ribonucleic acid nucleoporin 98 (circNUP98) is highly expressed in diabetic nephropathy (DN) patients and high glucose-stimulated human glomerular mesangial cells (HMCs). (a) The expression of circNUP98 in DN patients and normal control was detected using quantitative reverse transcription polymerase chain reaction (qRT–PCR). (b) qRT–PCR analysis of circNUP98 expression in high glucose (HG)- or normal glucose (NG)-stimulated HMC). (c) qRT–PCR analysis of circNUP98 and linear NUP98 expression in HMCs treated with actinomycin D. (d) qRT–PCR analysis of circNUP98 and linear NUP98 expression in HMCs treated with RNase R or mock. ***$P < 0.001$.

intracellular ROS level in HMCs treated with HG was high, whereas circNUP98 silencing reversed this condition (Figure 3d). In addition, MDA level and SOD activity represent the degree of oxidative stress damage to cells. It was proved that circNUP98 silencing abolished HG-induced MDA elevation and SOD decrease in HMCs (Figure 3e,f). In all, circNUP98 knockdown reduced HG-evoked inflammatory response and oxidative stress.

### MiR-151-3p is a target of circNUP98

Given that circRNAs located in the cytoplasm can act as sponges for miRNAs, we then first tried to investigate the subcellular localization of circNUP98. Subcellular fractionation assay showed that circNUP98 was mainly distributed in the cytoplasm of HMCs (Figure 4a). Next, miRNAs binding with circNUP98 were predicted through the use of the Circinteractome database, and 27 miRNAs were predicted to have the complementary binding sites on circNUP98 (Figure 4b), among which, only miR-151-3p and miR-136 were reported to be downregulated in DN, and might show inhibitory action in DN progression[16, 17]. Furthermore, the results of qRT–PCR suggested that circNUP98 knockdown significantly upregulated miR-151-3p expression, but not miR-136 in HMCs; thus, we speculated that miR-151-3p might be a target for circNUP98 (Figure S1c). The full length of circNUP98-wild-type and the mutant version without miR-151-3p binding sites were subcloned into luciferase reporter vector pmirGLO (Figure 4b). After the validation of the elevation efficiency of miR-151-3p mimic (Figure 4c), the dual-luciferase reporter assay was carried out. The results suggested that the luciferase activity of the wild-type circNUP98 reporter, but not the mutated one, was significantly reduced by miR-151-3p mimic in HMCs (Figure 4d). RNA pull-down assay showed that miR-151-3p was notably pulled down by biotin-labeled circNUP98 probe (Figure 4e). Furthermore, RIP assay showed that circNUP98 and miR-151-3p were significantly enriched in RNA complexes in the Ago2 group compared with the immunoglobulin G group (Figure 4f), further verifying the binding between circNUP98 and miR-151-3p. Additionally, miR-151-3p expression was increased by circNUP98 knockdown in HMCs (Figure 4g). Meanwhile, miR-151-3p expression was observed to be decreased in the serum of DN patients (Figure 4h), which was negatively correlated with circNUP98 expression (Figure 4i). Also, a marked decrease of miR-151-3p expression in HG-induced HMCs cells was detected (Figure 4j). Altogether, circNUP98 targeted miR-151-3p and negatively regulated its expression.

### CircNUP98 knockdown suppresses HG-induced HMC injury by targeting miR-151-3p

Subsequently, we carried out rescue experiments to further elucidate whether circNUP98 exerted its effects by adsorbing miR-

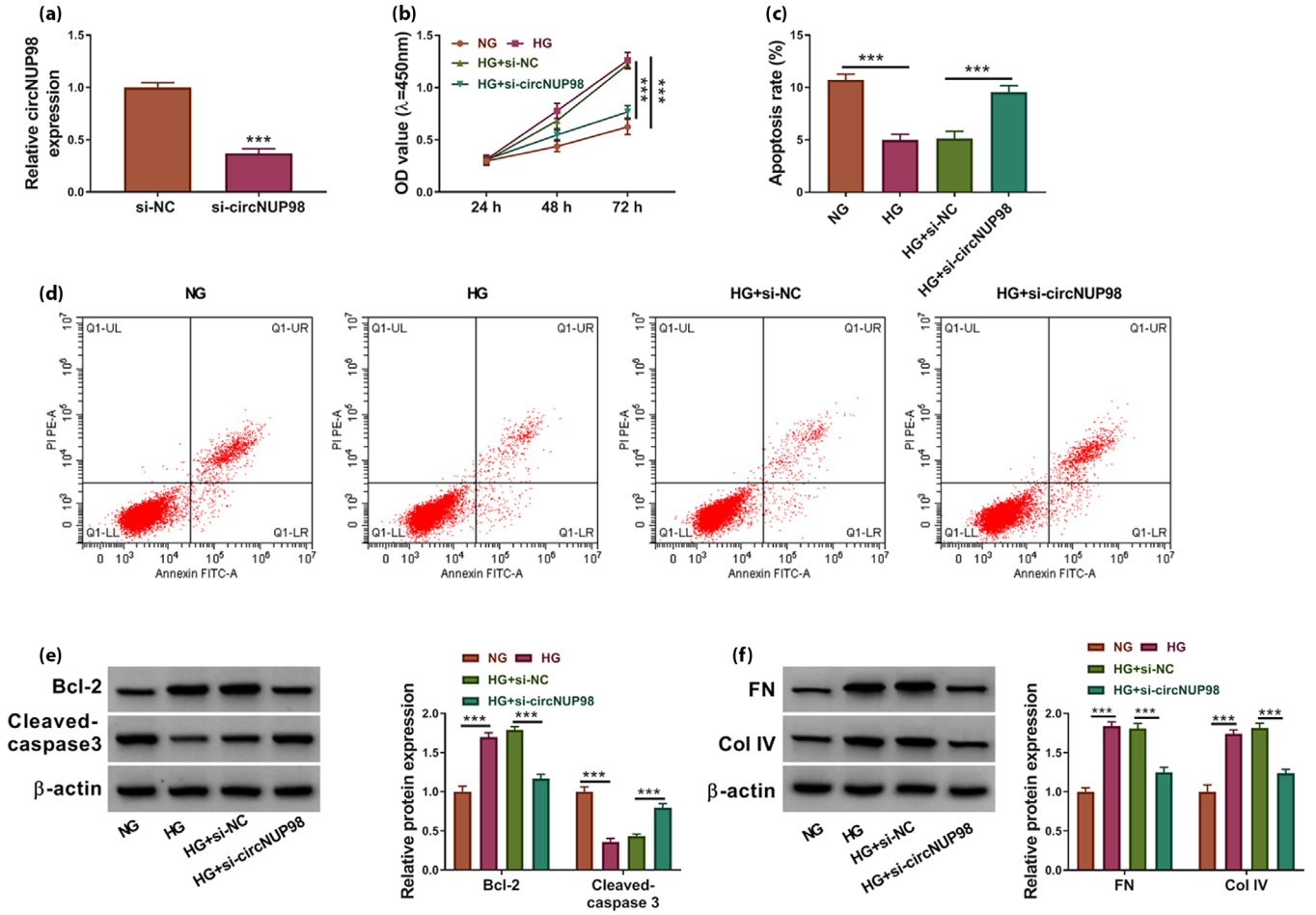


**Figure 2** | Circular ribonucleic acid nucleoporin 98 (circNUP98) knockdown suppresses proliferation and fibrosis in in high glucose (HG)-induced human glomerular mesangial cells (HMCs). (a) The knockdown efficiency of small interfering (si)-circNUP98 or si-negative control (NC) in HMCs was confirmed by quantitative reverse transcription polymerase chain reaction. (b–f) Transfected HMCs were subjected to HG treatment. (b) Cell counting kit-8 assay for cell proliferation. (c,d) Flow cytometry for cell apoptosis. (e,f) Western blot analysis for the protein levels of Bcl-2, Cleaved-caspase3, fibronectin (FN) and collagen IV (Col IV) in cells. ***$P < 0.001$.

151-3p. HMCs were co-transfected with circNUP98 siRNA and miR-151-3p inhibitor, and the results of qRT–PCR suggested that miR-151-3p inhibition reverted the upregulation of miR-151-3p caused by circNUP98 silencing in HMCs (Figure 5a). After the HG treatment, we discovered that miR-151-3p knockdown reversed the inhibitory influence of circNUP98 silencing on proliferation (Figure 5b) and promoting impact on apoptosis (Figure 5c–e) in HG-stimulated HMCs. Also, both the decreases of pro-fibrotic markers FN and Col IV mediated by circNUP98 silencing in HG-stimulated HMCs were restored by miR-151-3p downregulation (Figure 5f). In addition, miR-151-3p silencing reversed the circNUP98 silencing-triggered inhibition of inflammatory response (Figure 5g–i) and oxidative stress in HG-stimulated HMCs (Figure 5j–l). Collectively, the circNUP98–miR-151-3p axis was responsible for HG-induced HMC injury.

### HMGA2 is a target of miR-151-3p, and circNUP98 regulates HMGA2 by sponging miR-151-3p

To investigate the regulatory mechanism underlying miR-151-3p in HG-stimulated HMCs, we searched the targets of miR-151-3p through the Starbase database. MiR-151-3p possessed a potential binding site on HMGA2 (Figure 6a). The results of dual-luciferase reporter assay showed that miR-151-3p overexpression overtly declined the luciferase activity of the wild-type HMGA2 luciferase plasmid, but not the mutated one in HMCs (Figure 6b), suggesting the binding between miR-151-3p and HMGA2. In addition, miR-151-3p overexpression decreased the expression level of HMGA2 in HMCs (Figure 6c, d). All these data confirmed that miR-151-3p targetedly suppressed HMGA2 expression. Furthermore, HG treatment induced the elevation of HMGA2 expression levels (Figure 6e, f). CircNUP98 silencing reduced HMGA2 expression, which was rescued by miR-

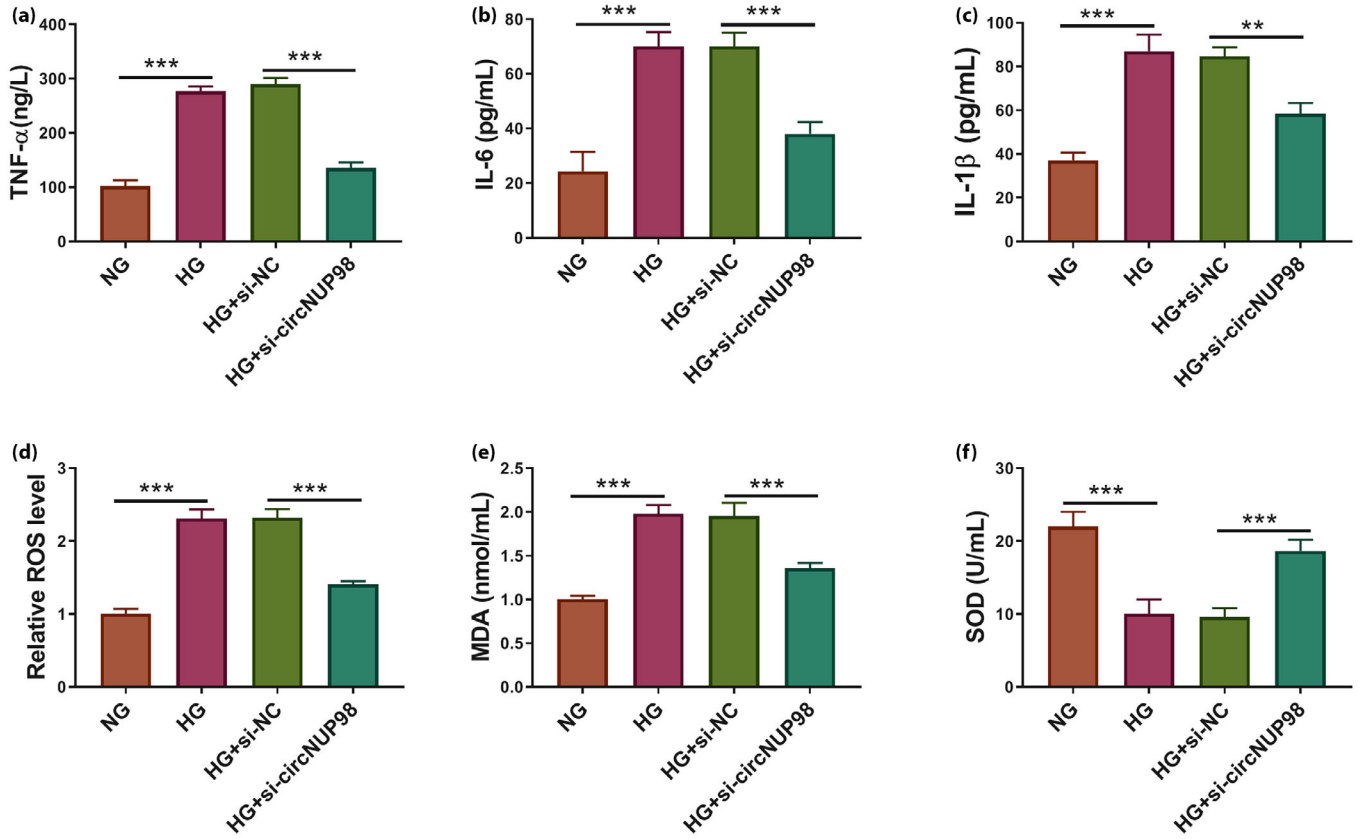


**Figure 3** | Circular ribonucleic acid nucleoporin 98 (circNUP98) knockdown suppresses inflammatory response and oxidative stress in high glucose (HG)-induced human glomerular mesangial cells (HMCs). (a–f) HMCs transfected with small interfering (si)-circNUP98 or si-negative control (NC) were subjected to HG treatment. (a–c) Enzyme-linked immunosorbent assay analysis of tumor necrosis factor (TNF)-α, interleukin (IL)-6 and IL-1β levels in cells. (d) Dihydroethidium staining for reactive oxygen species (ROS) production. (e,f) Malondialdehyde (MDA) production and superoxide dismutase (SOD) content were examined using corresponding commercial kits. $^{**}P < 0.01$, $^{***}P < 0.001$.

151-3p inhibition in HG-induced HMCs (Figure 6g, h). In addition, HMGA2 expression was increased in the serum of DN patients (Figure 6i, j), which was negatively correlated with miR-151-3p expression (Figure 6k), whereas it was positively correlated with circNUP98 expression (Figure 6l). Therefore, a circNUP98–miR-151-3p–HMGA2 feedback loop was identified in HMCs.

### MiR-151-3p re-expression suppresses HG-induced HMC injury by targeting HMGA2

Next, the effects of the miR-151-3p–HMGA2 axis on HG-stimulated HMCs were explored. After the introduction of HMGA2 overexpression vector, the downregulation of HMGA2 caused by miR-151-3p mimic was reduced in HMCs (Figure 7a). Thereafter, we found that miR-151-3p mimic induced proliferation arrest and apoptosis in HG-stimulated HMCs, which were attenuated by HMGA2 overexpression (Figure 7b–e). In addition, miR-151-3p mimic caused the decrease of FN and Col IV protein levels, as well as the inhibition of TNF-α, IL-6 and IL-1β release in HG-stimulated HMCs, whereas HMGA2 overexpression reversed these actions (Figure 7f-i). Furthermore, HMGA2 overexpression abolished miR-151-3p mimic-evoked reduction of ROS and MDA levels, as well as elevation of SOD content in HG-stimulated HMCs (Figure 7j–l). In all, miR-151-3p retrained HG-induced proliferation, fibrosis inflammatory response and oxidative stress in HMCs by HMGA2.

### CircNUP98 is packaged into exosomes

Exosomes are one of the vesicle types that mediated cell–cell communication through the transfer of their contents, which has been considered as an ideal therapeutic strategy for disease[18, 19]. To investigate the the clinical impact of of circNUP98, the origin of circNUP98 was determined in DN. TEM data verified exosome morphology (Figure 8a). Nanoparticle tracking analysis suggested the typical average exosome size distribution (Figure 8b), and the exosomal markers were detectable (Figure 8c). Thereafter, it was proved that circNUP98 is detectable in exosomes, and showed a high expression level in the exosomes isolated from DN patients (Figure 8d). Furthermore, the

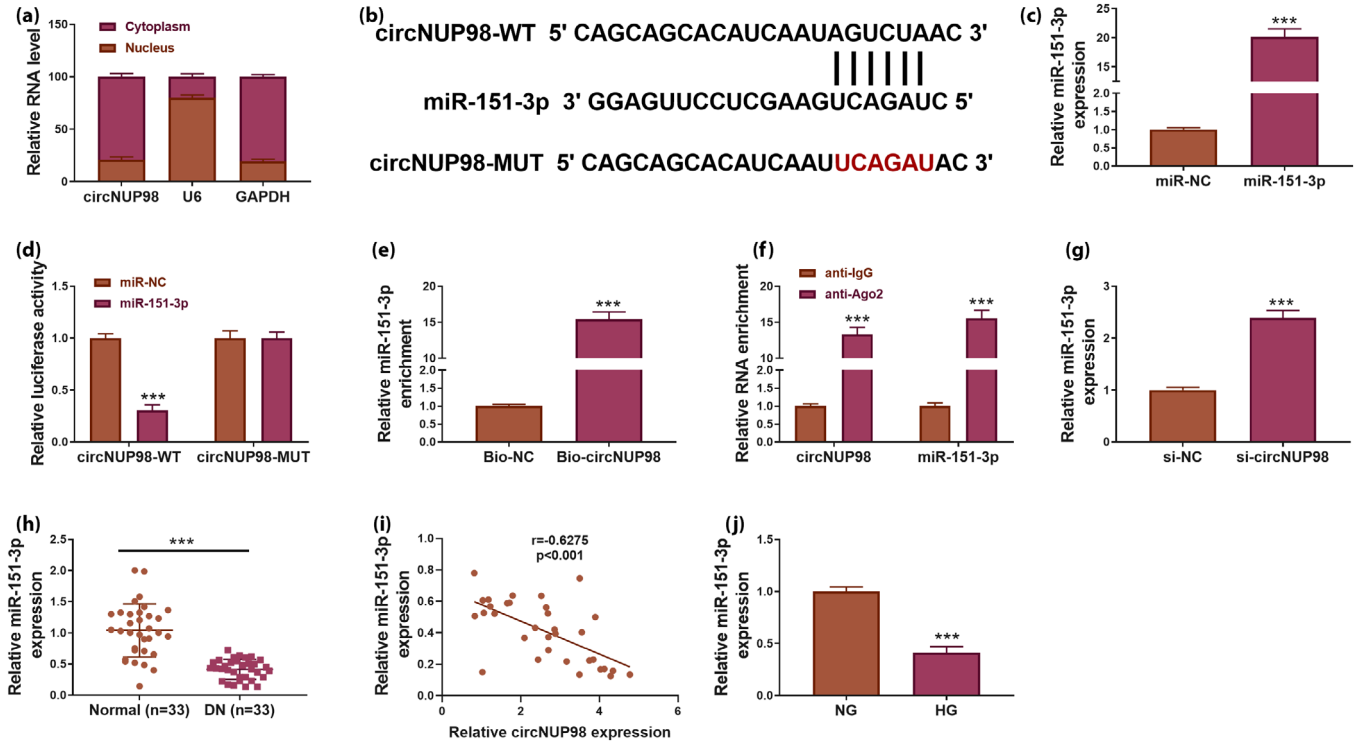


**Figure 4** | Microribonucleic acid (miR)-151-3p is a target of circular ribonucleic acid nucleoporin 98 (circNUP98). (a) Subcellular fractionation assay showing the distribution of circNUP98 in the cytoplasmic and nuclear fractions of human glomerular mesangial cells (HMCs). (b) The Circinteractome database showing the binding site of miR-151-3p with circNUP98, and the mutated sequence of circNUP98 in the binding site. (c) The elevation efficiency of miR-151-3p mimic or mimic negative control (NC) was validated by quantitative reverse transcription polymerase chain reaction (qRT–PCR). (d) Dual-luciferase reporter assay for the luciferase activity of wild and mutated circNUP98 reporter after miR-151-3p overexpression in HMCs. (e) Pull-down assay was carried out using the circNUP98-specific probe and control probe, and the enrichment of miR-151-3p was examined by qRT–PCR. (f) Radioimmunoprecipitation experiment was carried out with Ago2 antibody and negative control immunoglobulin G, followed by qRT–PCR to measure the levels of miR-151-3p and circNUP98. (g) qRT–PCR analysis of miR-151-3p expression in HMCs transfected with small interfering (si)-circNUP98 or si-NC. (h) The expression of miR-151-3p in diabetic nephropathy (DN) patients and normal controls was detected using qRT–PCR. (i) MiR-151-3p expression was negatively correlated with circNUP98 in DN patients. (j) qRT–PCR analysis of miR-151-3p expression in high glucose (HG)- or normal glucose (NG)-stimulated HMCs. ***$P < 0.001$.

receiver operating characteristic curve was carried out to evaluate the diagnostic value of exosomal circNUP98 in DN, the results showed an area under curve of 0.9146 (Figure 8e). These results suggested that circNUP98 was packaged into exosomes, and exosomal circNUP98 might be a promising diagnostic biomarker for DN.

## DISCUSSION

DN is one of the leading causes of end-stage chronic kidney disease[20]. In China, DN become the main cause of chronic kidney disease in the hospitalized population in 2015, with a substantially ascending rate doubling in the past decade[21]. EMC accumulation and microinflammation are common pathways for DN progression[22]. In addition, hyperglycemia-mediated dysregulation of diverse pathways reinforced the intensity of oxidative stress, which also induces the development of DN[23]. Currently, increasing evidence shows the involvement of circRNA in the pathogenesis of DN[12]. In the present study, circNUP98 was found to be upregulated in the blood of DN patients. Then, we used HG-stimulated HMCs to investigate the potential action of circNUP98 in the DN process. It was proved that HG treatment induced a significant elevation of circNUP98 expression level in HMCs. Functionally, we discovered that silencing of circNUP98 induced apoptosis and reduced proliferation in HG-stimulated HMCs. Both the elevation of the profibrotic factors FN and Col IV mediated by HG were confirmed to be reversed by circNUP98 silencing. Besides that, circNUP98 deletion reduced the release of pro-inflammatory cytokines TNF-α, IL-6 and IL-1β in HG-stimulated HMCs. Furthermore, its downregulation also decreased the production of ROS and MDA, but elevated the content of SOD in HG-stimulated HMCs. Thus, we showed that knockdown of circNUP98 might protect MCs from hyperglycemia-evoked injury.

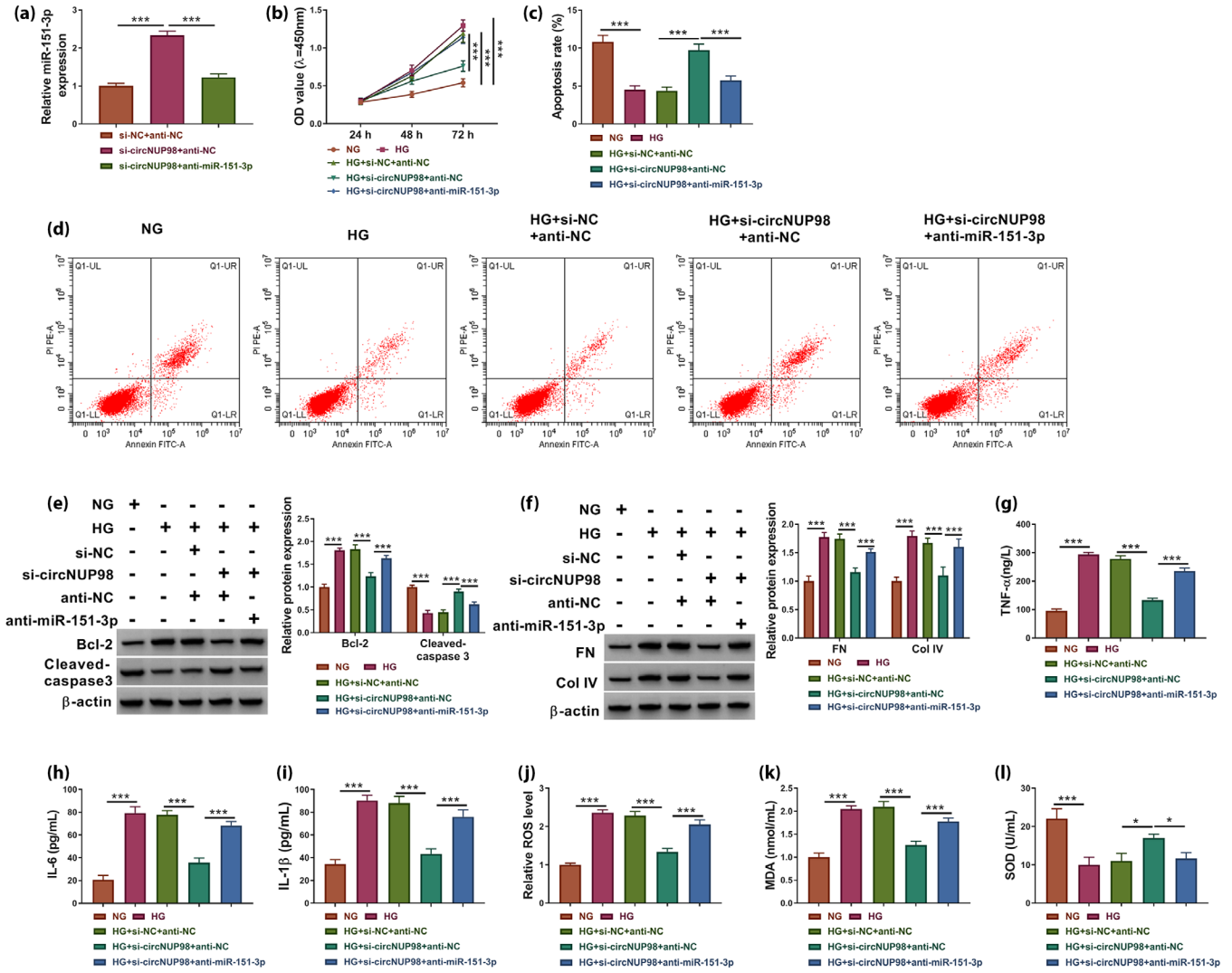


**Figure 5** | Circular ribonucleic acid nucleoporin 98 (circNUP98) knockdown suppresses high glucose (HG)-induced human glomerular mesangial cell (HMC) injury by targeting microribonucleic acid (miR)-151-3p. (a) HMCs were transfected with small interfering (si)- negative control (NC) + anti-NC, si-circNUP98 + anti-NC, or si-circNUP98 + anti-miR-151-3p, and the transfection efficiency was verified by detecting miR-151-3p expression using quantitative reverse transcription polymerase chain reaction. (b–l) Transfected HMCs were subjected to HG treatment. (c) Cell counting kit-8 assay for cell proliferation. (c,d) Flow cytometry for cell apoptosis. (e,f) Western blot analysis for the protein levels of Bcl-2, Cleaved-caspase3, fibronectin (FN) and collagen IV (Col IV) in cells. (g–i) Enzyme-linked immunosorbent assay analysis of tumor necrosis factor (TNF)-α, interleukin (IL)-6 and IL-1β levels in cells. (j) Dihydroethidium staining for reactive oxygen species (ROS) production. (k, l) Malondialdehyde (MDA) production and superoxide dismutase (SOD) content were examined using corresponding commercial kits. *$P < 0.05$, ***$P < 0.001$.

Previous studies have uncovered that circRNAs can serve as a competing endogenous RNA to sponge miRNAs, and subsequently repress their degradation on target mRNAs[24, 25]. MiRNAs are a kind of short (~ 22 nt) non-coding RNA, which are also shown to play vital roles in DN progression[26]. MiR-151-3p is a functional miRNA, which has been shown to exert anti-cancer effects on many types of cancers, such as colon cancer, breast cancer, ovarian cancer and so on[27–29]. In DN, An *et al.*[12] showed that miR-151-3p acted as a target of hsa_circ_0003928 to participate in hsa_circ_0003928-induced ROS overproduction and inflammatory response in human renal epithelial cells HK-2 under HG treatment. In the present study, we confirmed that circNUP98 directly sponged miR-151-3p. MiR-151-3p was observed to be decreased in DN patients and HG-induced HMCs. Subsequently, a series of functional experiments showed that miR-151-3p re-expression in HMCs attenuated HG-evoked proliferation, inflammatory response, fibrosis and oxidative stress in cells. Furthermore, miR-151-3p inhibition abolished the

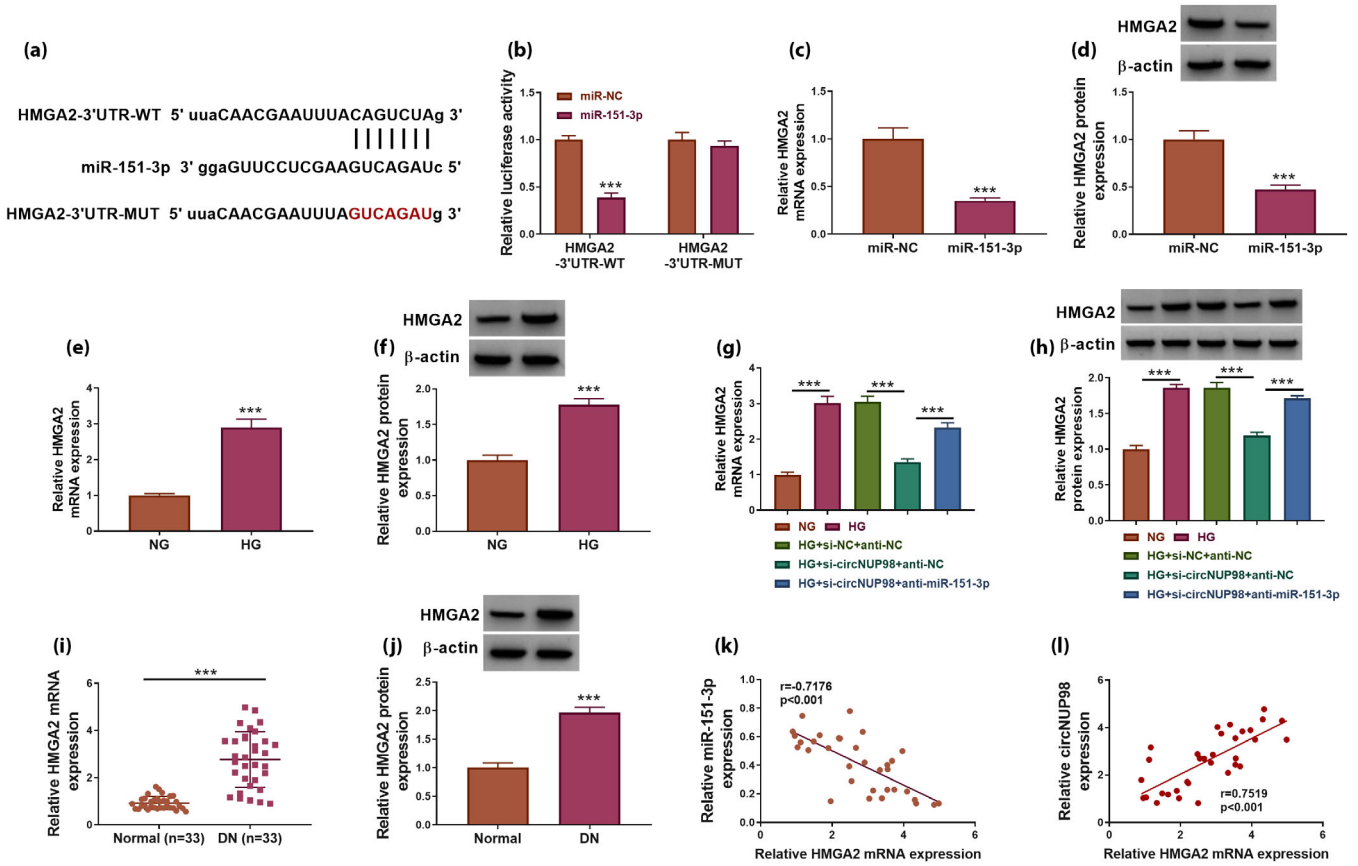


**Figure 6** | High mobility group AT-hook 2 (HMGA2) is a target of microribonucleic acid (miR)-151-3p, and circular ribonucleic acid nucleoporin 98 (circNUP98) regulates HMGA2 by sponging miR-151-3p. (a) The Starbase database showing the binding site of miR-151-3p with HMGA2, and the mutated sequence of HMGA2 in the binding site. (b) Dual-luciferase reporter assay for the luciferase activity of wild and mutated HMGA2 reporter after miR-151-3p overexpression in human glomerular mesangial cells (HMCs). (c,d) Quantitative reverse transcription polymerase chain reaction (qRT-PCR) and western blot analysis of HMGA2 level in HMCs transfected with miR-151-3p or miR-negative control (NC). (e,f) qRT–PCR and western blot analysis of HMGA2 level in HMCs treated with high glucose (HG) or normal glucose (NG). (g, h) qRT–PCR and western blot analysis of HMGA2 level in HMCs transfected with small interfering (si)-NC + anti-NC, si-circNUP98 + anti-NC or si-circNUP98 + anti-miR-151-3p in the presence of HG. (i, j) qRT–PCR and western blot analysis of HMGA2 level in diabetic nephropathy (DN) patients and normal control. (k) HMGA2 expression was negatively correlated with miR-151-3p expression in DN patients. (l) HMGA2 expression was positively correlated with circNUP98 expression in DN patients. ***$P < 0.001$.

inhibitory action of circNUP98 knockdown on HG-triggered HMC dysfunction. Additionally, we also verified that miR-151-3p targeted HMGA2; furthermore, circNUP98 acted as a sponge for miR-151-3p to positively regulate HMGA2 expression. HMGA2 is a well-recognized oncofetal protein, the overexpression of which is considered as a feature of malignancy[30]. Recent studies have documented that HMGA2 has effects on DN progression. For example, miR-98-5p prevented EMT process and renal fibrosis by targeting HMGA2[31]. Bai *et al.*[32] showed that HMGA2 silencing reduced advanced glycation end-products-evoked EMT and ROS production in tubular epithelial cells by activating the p38 mitogen-activated protein kinase pathway. In addition, let-7a-5p attenuated HG-induced MCs proliferation through blocking the phosphoinositide 3-kinase–protein kinase B pathway through HMGA2[33]. All these findings imply the promoting effects of HMGA2 on DN progression. In the present study, we found that HMGA2 upregulation abolished the protective functions of miR-151-3p on HG-induced HMCs. Thus, a functional circNUP98–miR-151-3p–HMGA2 axis in HMCs is identified.

Exosomes are important mediators of cell–cell communication through the transfer of their contents to exert their functions[18, 19]. In addition, exosomes are characterized by long half-life in circulation, low immunogenicity, low-risk for cancer formation and the ability to cross the blood–brain barrier; thus, exosomes are considered as ideal delivery vehicles for therapeutic drugs[18, 19]. In the current study, we found that circNUP98 was packaged into exosomes in the serum of DN patients. In

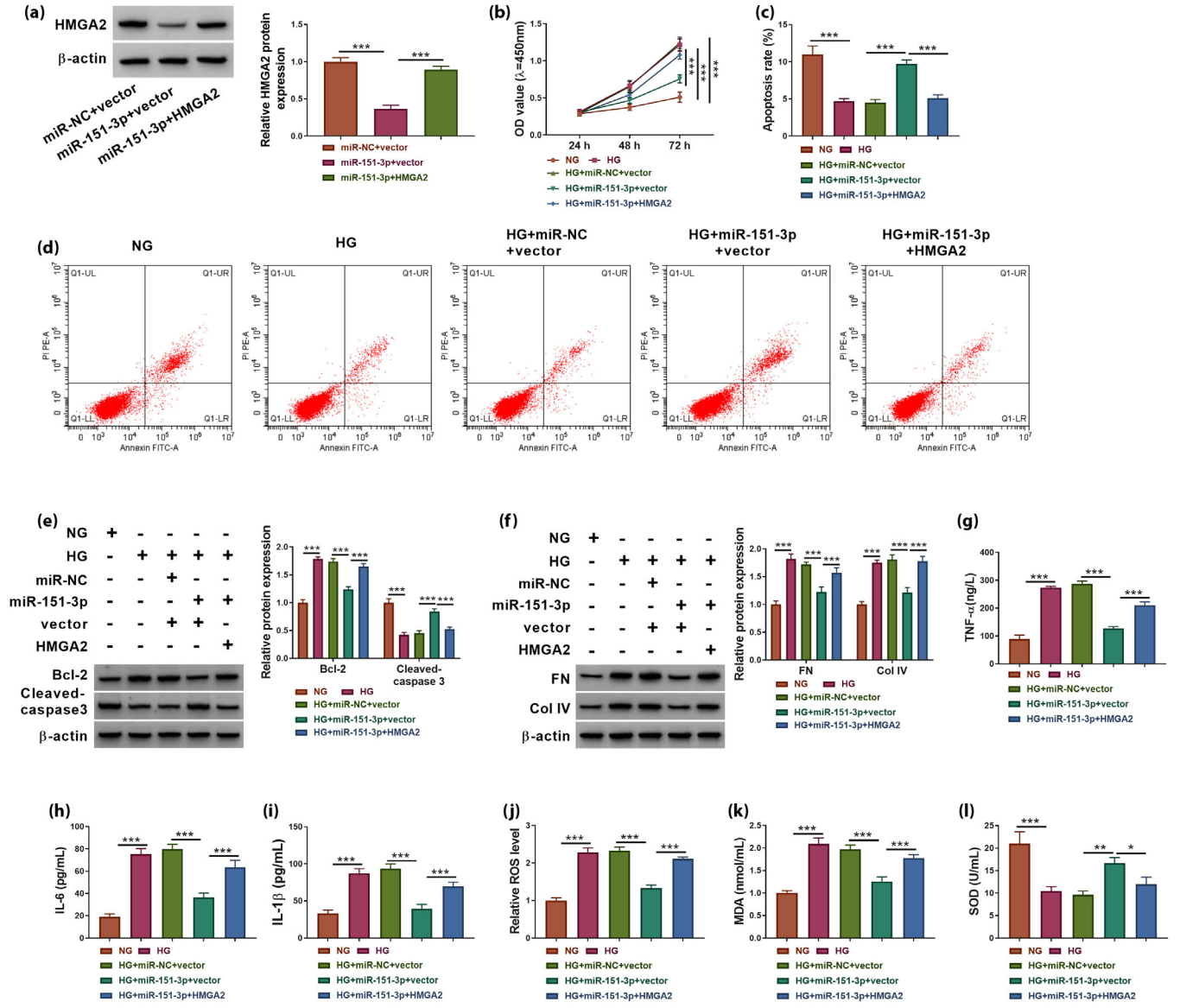


**Figure 7** | Microribonucleic acid (miR)-151-3p re-expression suppresses high glucose (HG)-induced human glomerular mesangial cell (HMC) injury by targeting high mobility group AT-hook 2 (HMGA2). (a) HMCs were transfected with miR-negative control (NC) + vector, miR-151-3p + vector or miR-151-3p + HMGA2, and the transfection efficiency was verified by detecting HMGA2 expression using western blot. (b–l) Transfected HMCs were subjected to HG treatment. (b) Cell counting kit-8 assay for cell proliferation. (c,d) Flow cytometry for cell apoptosis. (e, f) Western blot analysis for the protein levels of Bcl-2, Cleaved-caspase3, fibronectin (FN) and collagen IV (Col IV) in cells. (g–i) Enzyme-linked immunosorbent assay analysis of tumor necrosis factor (TNF)-α, interleukin (IL)-6 and IL-1β levels in cells. (j) Dihydroethidium staining for reactive oxygen species (ROS) production. (k, l) Malondialdehyde (MDA) production and superoxide dismutase (SOD) content were examined using corresponding commercial kits. *$P < 0.05$, ***$P < 0.001$.

addition, receiver operating characteristic curve analysis showed an area under curve of 0.9146 of exosomal circNUP98 in DN, suggesting the potential application of circNUP98 in clinic.

In all, this work for the first time showed that circNUP98 knockdown prevented HG-induced proliferation, fibrosis, inflammatory response and oxidative stress in HMCs by regulating the miR-151–3p/HMGA2 axis. Furthermore, circNUP98 was packaged into exosomes in the serum of DN patients, which suggested the therapeutic potential of circNUP98 in DN through exosomes.

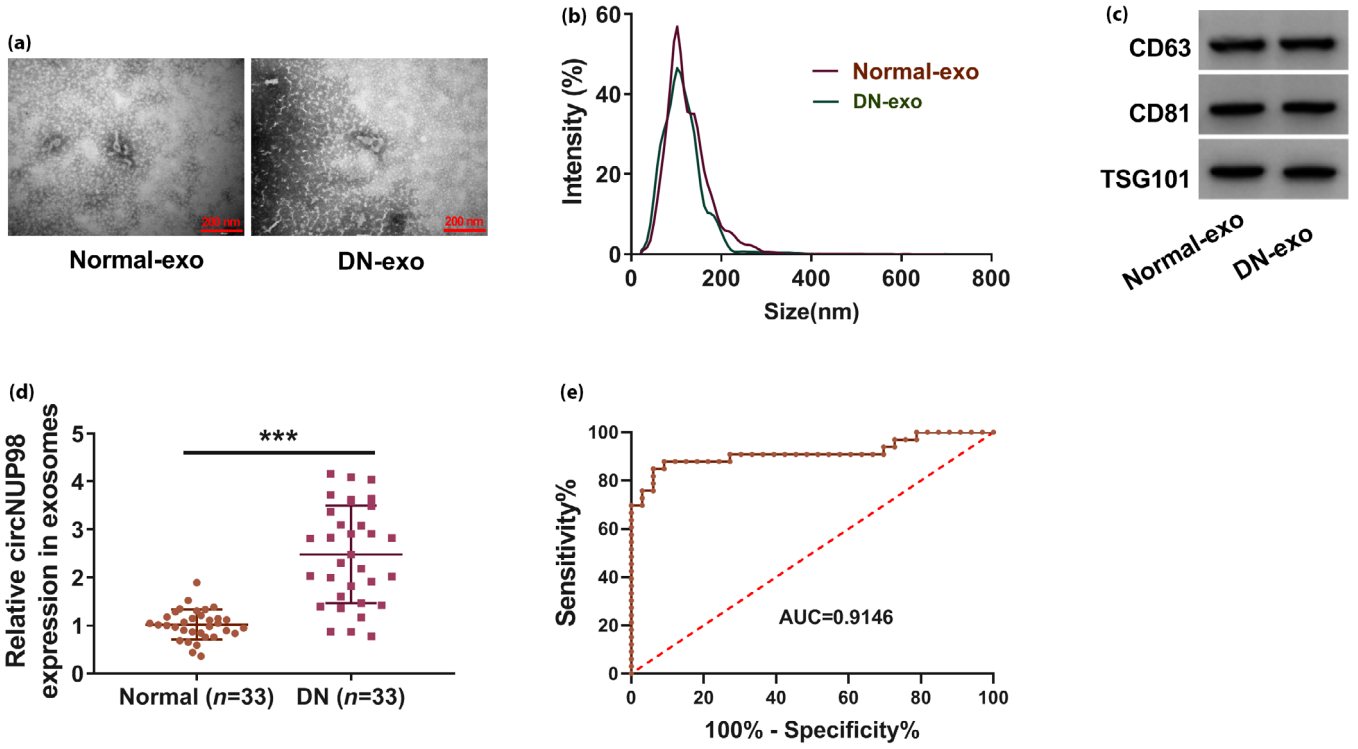


**Figure 8** | Circular ribonucleic acid nucleoporin 98 (circNUP98) is packaged into exosomes (exo). (a) Transmission electron microscopy images of exosomes isolated from the serum of diabetic nephropathy (DN) patients or normal control. (b) Exosome size distribution was determined by a nanoparticle tracking analysis. (c) Western blot analysis for exosomes markers CD63, TSG101 and CD81. (d) Quantitative reverse transcription polymerase chain reaction analysis of circNUP98 expression level in isolated exosomes. (e) Receiver operating characteristic curve analysis of the diagnostic value of exosomal circNUP98 in DN patients. ***$P < 0.001$.

## ACKNOWLEDGMENTS

This work was supported by Shaanxi Science and Technology Research and Development Project Fund (2017SF-263).

## DISCLOSURE

The authors declare no conflict of interest.

Approval of the research protocol: The present study was approved by the ethical review committee of Shaanxi Provincial People's Hospital. Written informed consent was obtained from all enrolled patients.

Informed consent: The patients agreed to participate in this work.

Registry and the registration no. of the study/trial: Approval date of Registry and the Registration No.20210216; Approval date: 16 February 2021.

Animal studies: Animal studies were carried out in compliance with the ARRIVE guidelines and the Basel Declaration. All animals received humane care according to the National Institutes of Health (USA) guidelines.

## REFERENCES

1. Qi C, Mao X, Zhang Z, *et al*. Classification and differential diagnosis of diabetic nephropathy. *J Diabetes Res* 2017; 2017: 8637138.
2. Maezawa Y, Takemoto M, Yokote K. Cell biology of diabetic nephropathy: roles of endothelial cells, tubulointerstitial cells and podocytes. *J Diabetes Investig* 2015; 6: 3–15.
3. Najafian B, Alpers CE, Fogo AB. Pathology of human diabetic nephropathy. *Contrib Nephrol* 2011; 170: 36–47.
4. Wang XB, Zhu H, Song W, *et al*. Gremlin regulates podocyte apoptosis via transforming growth factor-β (TGF-β) pathway in diabetic nephropathy. *Med Sci Monitor* 2018; 24: 183–189.
5. Chen C, Gong W, Li C, *et al*. Sphingosine kinase 1 mediates AGEs-induced fibronectin upregulation in diabetic nephropathy. *Oncotarget* 2017; 8: 78660–78676.
6. Chen LL, Yang L. Regulation of circRNA biogenesis. *RNA Biol* 2015; 12: 381–388.
7. Vo JN, Cieslik M, Zhang Y, *et al*. The landscape of circular RNA in cancer. *Cell* 2019; 176: 869–881 e813.
8. Kristensen LS, Andersen MS, Stagsted LVW, *et al*. The biogenesis, biology and characterization of circular RNAs. *Nat Rev Genet* 2019; 20: 675–691.
9. Wu J, Qi X, Liu L, *et al*. Emerging epigenetic regulation of circular RNAs in human cancer. *Mol Ther Nucleic acids* 2019; 16: 589–596.
10. Hua X, Sun Y, Chen J, *et al*. Circular RNAs in drug resistant tumors. *Biomed Pharmacother* 2019; 118: 109233.

11. Liu Y, Yang Y, Wang Z, *et al*. Insights into the regulatory role of circRNA in angiogenesis and clinical implications. *Atherosclerosis* 2020; 298: 14–26.
12. Zhang JR, Sun HJ. Roles of circular RNAs in diabetic complications: from molecular mechanisms to therapeutic potential. *Gene* 2020; 763: 145066.
13. Hu W, Han Q, Zhao L, *et al*. Circular RNA circRNA_15698 aggravates the extracellular matrix of diabetic nephropathy mesangial cells via miR-185/TGF-β1. *J Cell Physiol* 2019; 234: 1469–1476.
14. Peng F, Gong W, Li S, *et al*. circRNA_010383 acts as a sponge for miR-135a and its downregulated expression contributes to renal fibrosis in diabetic nephropathy. *Diabetes* 2021; 70: 603–615.
15. Yu R, Yao J, Ren Y. A novel circRNA, circNUP98, a potential biomarker, acted as an oncogene via the miR-567/ PRDX3 axis in renal cell carcinoma. *J Cell Mol Med* 2020; 24: 10177–10188.
16. Liu L, Pang X, Shang W, *et al*. miR-136 improves renal fibrosis in diabetic rats by targeting down-regulation of tyrosine kinase SYK and inhibition of TGF-β1/Smad3 signaling pathway. *Ren Fail* 2020; 42: 513–522.
17. An L, Ji D, Hu W, *et al*. Interference of Hsa_circ_0003928 alleviates high glucose-induced cell apoptosis and inflammation in HK-2 cells via miR-151-3p/Anxa2. *Diabetes Metab Syndr Obes: Targets Ther* 2020; 13: 3157–3168.
18. Yang Y, Ye Y, Su X, *et al*. MSCs-derived exosomes and neuroinflammation, neurogenesis and therapy of traumatic brain injury. *Front Cell Neurosci* 2017; 11: 55.
19. Kalani A, Tyagi A, Tyagi N. Exosomes: mediators of neurodegeneration, neuroprotection and therapeutics. *Mol Neurobiol* 2014; 49: 590–600.
20. Magee C, Grieve DJ, Watson CJ, *et al*. Diabetic nephropathy: a tangled web to unweave. *Cardiovasc Drugs Ther* 2017; 31: 579–592.
21. Zhang L, Long J, Jiang W, *et al*. Trends in chronic kidney disease in China. *N Engl J Med* 2016; 375: 905–906.
22. Wada J, Makino H. Inflammation and the pathogenesis of diabetic nephropathy. *Clin Sci*(London, England: 1979) 2013; 124: 139–152.
23. Arora MK, Singh UK. Oxidative stress: Meeting multiple targets in pathogenesis of diabetic nephropathy. *Curr Drug Targets* 2014; 15: 531–538.
24. Hansen TB, Jensen TI, Clausen BH, *et al*. Natural RNA circles function as efficient microRNA sponges. *Nature* 2013; 495: 384–388.
25. Thomson DW, Dinger ME. Endogenous microRNA sponges: Evidence and controversy. *Nat Rev Genet* 2016; 17: 272–283.
26. McClelland A, Hagiwara S, Kantharidis P. Where are we in diabetic nephropathy: microRNAs and biomarkers? *Curr Opin Nephrol Hypertens* 2014; 23: 80–86.
27. Yue C, Chen X, Li J, *et al*. miR-151-3p inhibits proliferation and invasion of colon cancer cell by targeting close homolog of L1. *J Biomed Nanotechnol* 2020; 16: 876–884.
28. Yeh TC, Huang TT, Yeh TS, *et al*. miR-151-3p targets TWIST1 to repress migration of human breast cancer cells. *PloS One* 2016; 11: e0168171.
29. Huang K, Liu D, Su C. Circ_0007841 accelerates ovarian cancer development through facilitating MEX3C expression by restraining miR-151-3p activity. *Aging* 2021; 13: 12058–12066.
30. Zhang S, Mo Q, Wang X. Oncological role of HMGA2 (review). *Int J Oncol* 2019; 55: 775–788.
31. Zhu Y, Xu J, Liang W, *et al*. miR-98-5p alleviated epithelial-to-mesenchymal transition and renal fibrosis via targeting Hmga2 in diabetic nephropathy. *Int J Endocrinol* 2019; 2019: 4946181.
32. Bai YH, Wang JP, Yang M, *et al*. SiRNA-HMGA2 weakened AGEs-induced epithelial-to-mesenchymal transition in tubular epithelial cells. *Biochem Biophys Res Commun* 2015; 457: 730–735.
33. Wang T, Zhu H, Yang S, *et al*. Let-7a-5p may participate in the pathogenesis of diabetic nephropathy through targeting HMGA2. *Mol Med Rep* 2019; 19: 4229–4237.

## SUPPORTING INFORMATION

Additional supporting information may be found online in the Supporting Information section at the end of the article.

**Figure S1** | (a) Quantitative reverse transcription polymerase chain reaction analysis of circular ribonucleic acid nucleoporin 98 expression in human glomerular mesangial cells exposed to high glucose or normal glucose treatment for 0, 12, 24,or 48 h. (b) The knockdown efficiency of small interfering circular ribonucleic acid nucleoporin 98 or small interfering negative control in human glomerular mesangial cells under high glucose treatment was confirmed by quantitative reverse transcription polymerase chain reaction. (c) The effects of circular ribonucleic acid nucleoporin 98 knockdown on microribonucleic acid-151-3p and microribonucleic acid-136 expression profiles. $^{**}P < 0.01$, $^{***}P < 0.001$.